Journal of Zhejiang University-SCIENCE A (Applied Physics & Engineering)
ISSN 1673-565X (Print); ISSN 1862-1775 (Online)
www.zju.edu.cn/jzus; www.springerlink.com
E-mail: jzus@zju.edu.cn

Development of the applicability of simplified Henry's method for skewed multicell box-girder bridges under traffic loading conditions

Iman MOHSENI, A. R. Khalim RASHID

(*Department of Civil Engineering, Universiti Kebangsaan Malaysia (National University of Malaysia), UKM Bangi, Selangor 43600, Malaysia*)

E-mail: mohseni@eng.ukm.my; khalim@eng.ukm.my

Received Apr. 15, 2012; Revision accepted July 16, 2012; Crosschecked Nov. 16, 2012

Abstract: Concrete precast multicell box-girder (MCB) bridges combine aesthetics with torsional stiffness perfectly. Previous analytical studies indicate that currently available specifications are unable to consider the effect of the twisting moment (torsional moment) on bridge actions. In straight bridges the effect of torsion is negligible and the transverse reinforced design is governed by other requirements. However, in the case of skewed bridges the effect of the twisting moment should be considered. Therefore, an in-depth study was performed on 90 concrete MCB bridges with skew angles ranging from 0° to 60°. For each girder the bridge actions were determined under the American Association of State Highway and Transportation Officials (AASHTO) live load conditions. The analytical results show that torsional stiffness and live load positions greatly affected the bridges' responses. In addition, based on a statistical analysis of the obtained results, several skew correction factors are proposed to improve the precision of the simplified Henry's method, which is widely used by bridge engineers to predict bridge actions. The relationship between the bending moment and secondary moments was also investigated and it was concluded that all secondary actions increase with an increase in skewness.

Key words: Distribution factor, Live loads, Skewed bridges, Grillage analysis
doi:10.1631/jzus.A1200098 **Document code:** A **CLC number:** TU37

1 Introduction

The use of multicell box-girder (MCB) bridges has increased progressively in recent years due to natural geographical constraints, man-made obstacles, space limitations and mountains terrains. Various analytical and numerical methods, such as the orthotropic plate theory (Heins, 1978), grillage analysis (Jaeger and Bakht, 1982) and finite element method, have been developed to compute the different structural actions of bridges. In addition, new formulae and simplified methods have been proposed by researchers for bridge design specifications to predict the distribution of wheel load as a major component of bridges. The American Association of State Highway and Transportation Officials (AASHTO, 2002) presented the simple "s-over" approach for determining live load distribution factors (LDFs) without considering the effect of skewness. The AASHTO load and resistance factor design (LRFD) specifications (AASHTO, 2008) defined more accurate and complicated LDF formulae for various types of bridge based on the results of the National Cooperative Highway Research Program (NCHRP) project 12-26 (Zokaie *et al*., 1993). The AASHTO LRFD specifications contained several skew correction factors (SCFs) specifications for different types of bridge in order to consider the skew effect on the shear and moment distribution of wheel loads.

The complexity of the formulae and the ranges of applicability set out in the AASHTO LRFD can be problematic in design procedures, so in many instances Henry's simplified equal distribution factor (EDF) method has been used to determine the lateral load distribution on girders (Huo *et al*., 2003). The

EDF method assumes that all beams have an equal distribution of live load effect. Huo *et al*. (2003) concluded that the EDF method accurately calculates the LDF of straight bridges and that the results are slightly greater than those from the finite element analysis and are within a reasonable range of the values of the AASHTO LRFD specifications. To improve the accuracy of the EDF method by considering the effect of continuity and skewness, several modification factors have been proposed (Zhang, 2008). In addition, the AASHTO LRFD specifications (AASHTO, 2008) live (LDF) equations were deduced using a grillage analysis of a large number of prototype bridges, neglecting the effects of torsion distribution on this factor.

Clearly, skewness exacerbates the torsion moment on bridges as it is directly dependent on the stiffness of the girders (Chun, 2010). Neglecting the effect of torsion on the distribution of wheel loads on the superstructure, as assumed in the development AASHTO LRFD specifications, may result in unsafe values, such as underestimations of the distribution factor of live loads on the girders.

Several extensive investigations have been performed to consider the effects of torsion, shear lag and distortion in box beam elements and to propose adequate intermediate diaphragm spacing to control the distortion of box girders (Razaqpur and Li, 1991; Fan and Helwig, 2002; Park *et al*., 2005). It has been concluded that skewness greatly intensifies the torsion distribution at the obtuse corner of skewed bridges, especially when vehicles are located near the corner.

However, due to the closed geometry of box-girders, large torsional stiffness results in a high Saint-Venant component and the effects of torsional warping are indeed insignificant (Kolbrunner and Basler, 1969; Begum, 2010). A computer program was developed to resolve the problem associated with torque applied on pre-stressed straight MCB using a softened truss model theory but it is not applicable to skewed bridges because the skewness effect was ignored (Fu and Tang, 2001).

The aims of this study were two-fold: firstly, to examine the behaviour of skewed MCB bridges in bending torsion, especially at the obtuse corner of the superstructure, with the objective of evaluating the efficiency of different parameters, such as the skew angle, torsional stiffness and number of boxes, on the distribution of live load on the girders, and secondly, to improve the accuracy of Henry's simplified EDF method. A parametric analysis of a hundred prototype cast-in-place MCB bridges was performed to establish several skew correction factor equations. Most bridges examined in this study were simple supported bridges and the selected skew angle varied from 0° to 60°.

2 Geometric and structural properties

Ninety prototype cast-in-place concrete MCB bridges with various configurations were analyzed, subjected to traffic loading condition. The length of span L, skew angle θ, number of boxes N_B, width of deck W, and number of lanes load N_L were variable depending on the geometry of the bridges. The typical cross sectional symbols are shown in Fig. 1, where d' and d'' are the top and bottom thickness of bridge deck, respectively, t_w is the web thickness, and B and d indicate the girder spacing and bridge depth, respectively. Table 1 shows the cross sectional properties of the bridges investigated.

The Ontario method (CHBDC, 2000), i.e., α-θ method, was used to develop the bridge database (Table 1) and the finding that the most economical and practical range of span-to-depth ratio is between 21 and 25 was used in developing the databases (Heins, 1978; Hall *et al*., 1999). There were no intermediate diaphragms between the supports, as the bridge analyses provide relatively conservative results for LDF (Tobias *et al*., 2004; Bae and Oliva, 2012). Most bridges considered in this study were simply supported. For bridges, the modulus of elasticity E of concrete and Poisson's ratio v are 22.90 GPa and 0.20, respectively.

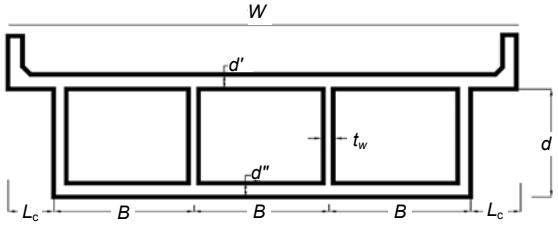

Fig. 1 Cross section symbols for a prototype multicell box-girder bridge

Table 1 Parameters considered in the analysis

Set	L (m)	N_B	N_L	W (m)	d' (mm)	d'' (mm)	θ (°)
1	30, 45, 60, 75, 90	2, 3	1, 2	9.10	0.20	0.15	0°, 30°, 45°, 60°
2	30, 45, 60, 75, 90	2, 3, 4	2, 3	14.0	0.20	0.15	0°, 30°, 45°, 60°
3	30, 45, 60, 75, 90	3, 4, 5, 6	2, 3, 4	17.0	0.20	0.15	0°, 30°, 45°, 60°

3 Bridge numerical modeling

3.1 Selected refined model

The behaviour of concrete MCB bridges was investigated using two different types of refined methods: orthogonal grillage and the finite element method. To determine the accuracy of grillage methods for various bridge actions, their results were compared with those from finite element analysis (FEA).

3.2 Bridge modeling technique

The commercially available finite element program CSIBRIDGE Version 15 was applied to the 3D modelling of the prototype bridges. A four node 3D shell element with six degrees of freedom at each node was used to model the prototype MCB bridges. The top and bottom shell elements of the web were integrated with the top and bottom slabs at the connection point to ensure compellability of deformation. The transverse solid diaphragms at the supports were modelled using the same element with the size and properties of the designed diaphragm (Huo *et al*., 2005).

Orthogonal grillage arrangements have been accepted as simple and reliable methods of analysis by many specifications (Jaeger and Bakht, 1982; Hambly, 1991; AASHTO, 2008). For skewed decks, transverse members are set as orthogonal to the longitudinal members to find out the most genuine moment and shear distribution. Although this model does indeed obtain acceptable results for skew bridges, due to some limitations in setting the grid member spacing, many researchers prefer to use the non-orthogonal grillage method. The grillage model was defined according to the rules described in Appendix A. Fig. 2 illustrates the typical form of all the described models, where m_x and m_y are the longitudinal and transverse bending moments that are obtained in elastic analysis, respectively, m_{xy} is the associated torsional moment whereas m_L and m_T are the bending moments that are required to design concrete MCB reinforcement oriented in the longitudinal and transverse directions, respectively.

Note that in the grillage models, the coupling of flexural bending in the main directions (M_x and M_y in Fig. 2) due to Poisson's ratio cannot be determined.

However, the contribution of the transverse bending moment in the longitudinal distribution is underestimated (Théoret *et al*., 2012). In addition, in the case of skewed bridges, the longitudinal and transverse torsions (T_L and T_T) and bending moments (M_L and M_T), respectively, must be transformed in the x-y coordinate system to calculate the adequate reinforcement, and L_s is slab width B projected in the longitudinal direction.

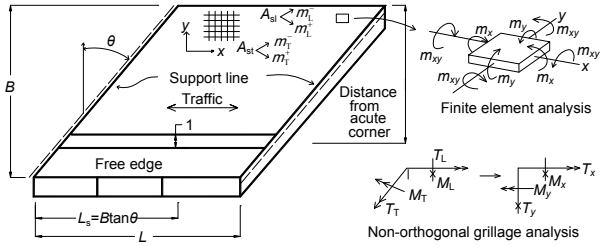

Fig. 2 Bridge geometry and moment definition

4 Support conditions

Boundary conditions were carefully evaluated to avoid unwanted constraints to the node and consequently for model. The number of constraints required to provide stability to the bridge model was kept to the minimum possible, bearing in mind that actual bridge behavior and performance had to be achieved. The boundary condition adopted in this study is similar to that used by Ashebo *et al*. (2007). All girders at the initial abutment were constrained to translate in all directions and the roller bearing was created at other supports. The rotation of supports around the X-direction (perpendicular to longitudinal direction) was restrained by the construction of appropriate solid concrete end diaphragms. Thus, the effect of end diaphragms was considered in the development of the skew correction factors for MCB bridges.

5 Verification of refined methods

The finite element method was verified by comparing the computed and measured bending moments, first natural frequencies and strain of the Tsing Yi Bridge in Hong Kong, China (Ashebo *et al*., 2007). The good agreement between the analytical and measured data showed that the same modelling method was suitable for analysis of skewed MCB bridges.

The example problem 5.5 from Hambly (1991) was selected for the verification grillage modelling of MCB bridges. The small differences of about 5% between the two approaches for longitudinal and transverse bending moments indicated that the modelling method was valid.

6 Loading condition

The traffic loading condition used in this study was the HL 93 bridge live load, which consists of the design truck (HS 20-44) plus design lane loads, or the design tandem plus design lane loads, whichever governs.

The multiple present factors of 1.00, 0.85, and 0.65 for two-, three-, and four-lane load conditions, respectively, were applied. A minimum distance of 60 cm was maintained between the first wheel loads and the curb edges of the bridge. Live loads were moved in both longitudinal and transverse directions of the bridge to obtain the maximum responses.

The truck and tandem positions in the transverse direction were chosen based on the number of lanes (Fig. 3). The minimum permitted distance between two adjacent vehicles was 1.20 m (AASHTO, 2008).

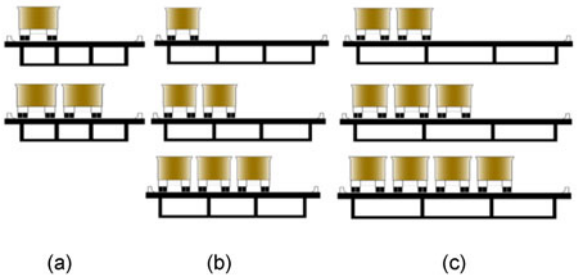

Fig. 3 Position and maximum number of trucks and tandems in the transverse direction of prototype bridges
(a) Two lanes; (b) Three lanes; (c) Four lanes

7 Live load distribution factor

The lateral distribution of the live load is a major parameter in the design and control of bridges. The live LDF is commonly obtained as follows (Barker and Puckett, 1997; AASHTO, 2002):

$$\mathrm{LDF}=\frac{F_{\mathrm{refined}}}{F_{\mathrm{beamline}}}, \tag{1}$$

where F_{refined} corresponds to the largest live loads in the girder from the refined methods, and F_{beamline} corresponds to the maximum live loads from a simple beam-line model subjected to one lane of traffic. To determine the LDF of MCB bridges, the cross section was idealized to an equivalent I-beam including one web, as well as bottom and top flanges. According to Eq. (1), the distribution factor of bridge actions, such as bending moment, shear, reaction and torsional moments, were obtained by dividing the maximum response of the finite element methods or grillage analysis, by the largest response from one of the idealised girders with a single lane of traffic.

Sennah and Kennedy (1999) indicated that the stiffness of a composite cellular structure depends on the thickness of the steel plates and deduced several expressions for torsional stiffness (J) for this type of bridge.

To develop an expression for the torsional stiffness of concrete MCB cross sections, the effect of the number of boxes, N_{B}, on torsional stiffness was investigated. There are two ways to determine the torsional stiffness, J, of MCB bridges, the precise method (simultaneous equations method) and the approximation method, in which the effect of the internal web is neglected in computing the torsional stiffness. Fig. 4 shows the variation in torsion-to-flexural stiffness ($GJ/(EI)$) versus the number of boxes (N_{B}). It became clear that internal webs have an insignificant effect on the distribution of shear flow over the cross section.

The approximation method calculated torsional stiffness up to 7% higher than the exact method. Therefore, the following simplified expression obtained by Sennah and Kennedy (1999) was used to determine the torsional stiffness of the prototype bridges. The membrane analysis method was used to deduce the following expression for three and four

cell-box cross sections, which is used in the parametric study:

For a three-box bridge:

$$J=\frac{4z^2d'(3X+10Y)}{X^2+4XY+2Y^2}; \tag{2}$$

For a four-box bridge:

$$J=\frac{8z^2d'(2X+5Y)}{X^2+3XY+Y^2}, \tag{3}$$

where $X=B[1+(d'/d'')]$, $Y=d[(d'/t_w)]$, and $Z=Bd$.

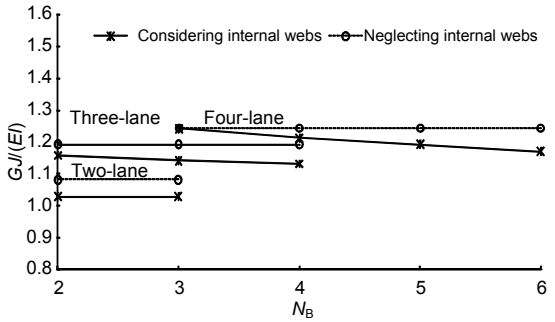

Fig. 4 Relationship between the number of boxes and the ratio of torsional-to-flexural rigidity

8 Effect of torsional rigidity

In bridge design procedures, although the influence of torsional moment on determining design actions is underestimated, the twisting moment induces transverse and negative moments and shear of skewed bridges that must be considered (Théoret *et al.*, 2012). One of the main aims of this study was to evaluate the influence of torsion on the bending moment and shear distribution in skewed bridges. Preliminary studies indicated that changing concrete slab thickness, span-to-depth ratio and top and bottom flange thickness does not have significant effects on skewed bridge actions (Huo *et al.*, 2003; Song *et al.*, 2003). However, it is obvious that torsional and flexural rigidity of bridges intensifies the effects of the above parameters.

Torsion induces the bending moment and shear in skewed bridges under traffic loading conditions. Subjected to flexural loading, the multicell box section deflects stiffly (longitudinal flexure) and deforms (normal distortion). Under twisting loading, the box section rotates rigidly and deforms (warping distortion). If intermediate diaphragms of adequate size and number are provided, the effects of sectional distortion can be disregarded.

Fig. 5 shows the influence of torsional stiffness J, on the bending moment, shear and twisting moment of skewed bridges. The results are presented as a function of the ratio of the bending moment, shear and torsion in skewed bridges to the corresponding straight bridge values.

Four levels of torsional stiffness corresponding to: (1) ultimate limit state (ULS), (2) serviceability limit state (SLS), (3) an arbitrary value (20% of J), and (4) torsion-less state, were applied. In the case of SLS, un-cracked stiffness was assumed, whereas in the ULS condition, it was assumed that the bridge's decks were severely cracked and then only 50% of the torsional stiffness was applied (Euro-Code 2, 2005; AASHTO, 2008).

Fig. 5a indicates that torsional stiffness has a negligible effect on the positive bending moment (maximum 10%). Thus, additional reinforcement in the longitudinal direction to prevent cracks developing is unnecessary.

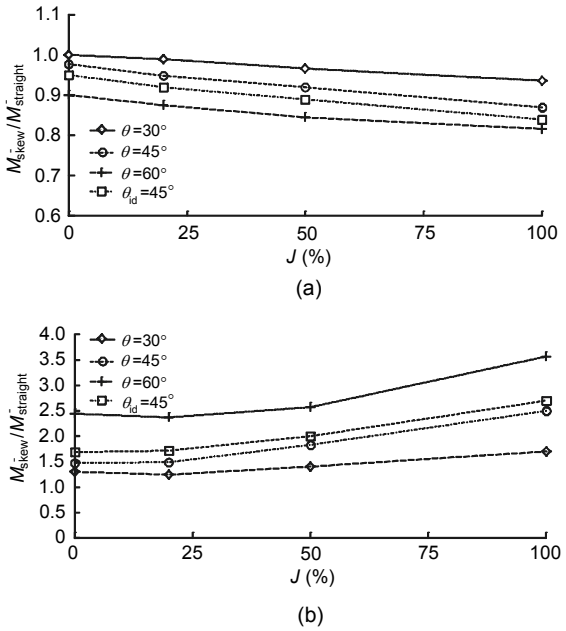

Fig. 5 Effect of torsional stiffness on maximum positive bending moment (a) and negative moment (b) at intermediate support

The effects of torsional stiffness on the negative bending moment are shown in Fig. 5b. The maximum 3.6 for the ratio M_{skew}/M_0 revealed about a 32% reduction in negative flexural bending in a case with a 60° skew angle. Great attention was paid to the obtuse corner of the skewed bridges where the maximum negative moment and shear are observed. Therefore, additional reinforcement was provided at this location to prevent crack development.

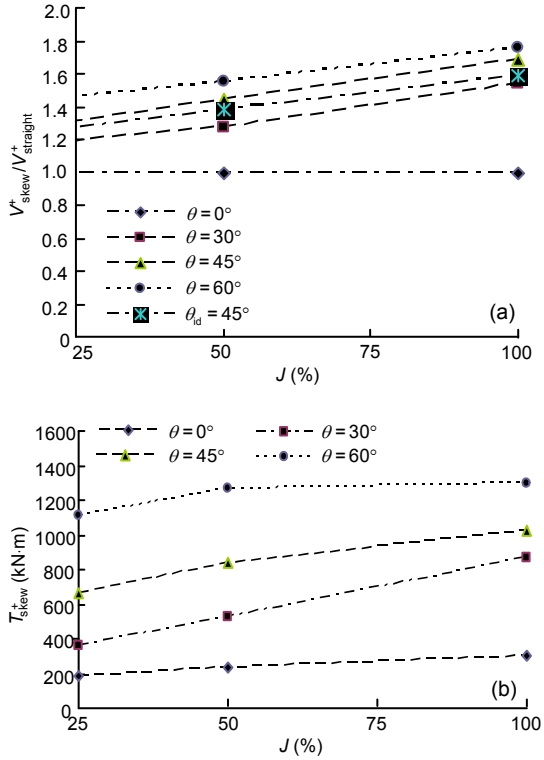

Fig. 6 Effect of shear stiffness (a) and torsional stiffness (b) on distribution of live load

For skewed bridges, the maximum shear accrues in the external girders at the obtuse corner (Huo and Zhang, 2008). In the serviceability limit state condition, the maximum shear is obtained. However, with decreasing torsional stiffness, the maximum shear for lower skew angles tends to occur in the first internal girder (Fig. 6a). With an increase in skewness, the positive bending moment near the mid-span decreases and the negative bending moment near the supports increases.

In addition, the maximum torsional moment of skewed and straight bridges (S_{skew} and $S_{straight}$) occurs in different girders due to the location of wheel loads on the superstructure, so drawing charts as a function of $S_{skew}/S_{straight}$ may lead to anomalous results. Hence, Fig. 6b was plotted based on the relationship between torsional stiffness and the positive torsion at the exterior girders for different skew angles.

Fig. 6 indicates that positive torque decreases with reducing torsional stiffness, by up to 22% with a skew angle of 60°. Diagonal cracking due to exceeding the diagonal principal tension from tensile strength is the main cause of this reduction; nevertheless, after cracking, the post cracking behaviour, such as tension-softening in both reinforced and unreinforced concrete regions is considerable. Unfortunately, the majority of finite element programs are unable to take into account this phenomenon during bridge analysis (Krätzig, 1993).

The effect on the bridge response of the presence of the intermediate diaphragms was also evaluated. Figs. 5 and 6 indicate that the variation in bending moment and shear of prototype MCB bridges with intermediate diaphragms (IDs) marginally improves. Similar improvement is observed for torsion distribution on the superstructure. The same finding has been observed in other studies (Zokaie *et al.*, 1993; Foinquinos *et al.*, 1997; Huo *et al.*, 2005).

9 Longitudinal distribution of twisting moment on girders

The distribution of torsion on the girders for a four-boxes MCB bridge with span length of 60 m and skew angle of 30°, subjected to AASHTO truck (HS 20-44) located at the midspan of the first lane (right side) of deck, was investigated. The distribution of twisting moment for exterior girder and three interior girder (interior 1, interior 2 and interior 3) are drawn in Fig. 7. It can be observed that the distribution of twisting depends on the distance from the center of gravity of the truck and girders. The maximum positive twisting moment occurred at the obtuse corner of the first intermediate girder at a distance of 2.90 m from the center of gravity of the live load. Consequently, the middle and third girders received a lower proportion of the total twisting moment. However, the maximum negative twisting moment was obtained at the acute corner of the right external girder (at a distance of 0.60 m from the truck), and was significantly higher than the negative twisting moment of the other girders.

In addition, when driving the design trucks to the right of their respective lanes, it was observed that the positive torque at the obtuse corner was reduced and that the negative torque at the acute corner was increased. Similar results were obtained when increasing the number of trucks in the transverse direction.

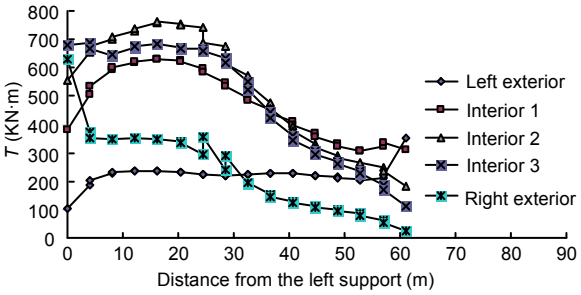

Fig. 7 Distribution of twisting moment in the longitudinal direction on skewed bridges

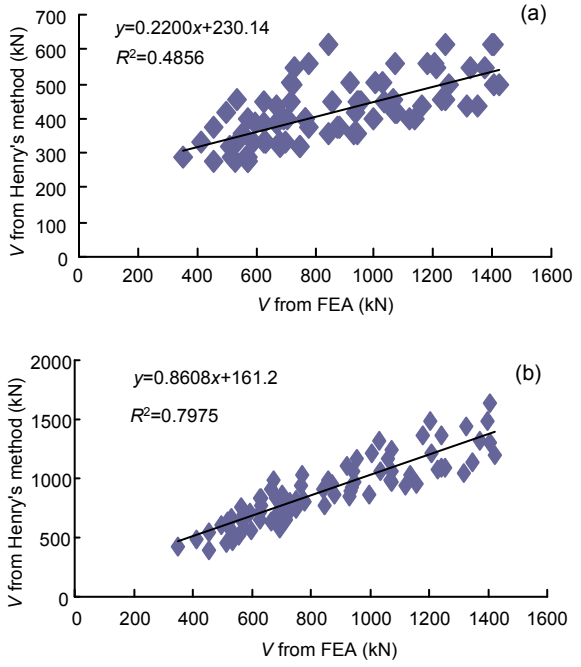

Fig. 8 Relationship between vertical shear force (V) determined by finite element analysis and by Henry's method, without (a) and with (b) the use of a skew correction factor

10 Improving simplified Henry's method

The AASHTO LRFD specification adopted the results of the NCHRP Project 12-26 (Zokaie *et al*., 1993) to determine the live LDF of different types of bridges. Although these formulae predict more accurate LDF values, their complexity and limitations often deter their use by bridge engineers. Hence, in many bridge design procedures, LDF are determined using other simplified and easier methods, such as Henry's EDF method, which requires only the width of roadway and the number of webs to calculate the LDF of bridges (Appendix B).

Nevertheless, only a few studies have taken into account the effect of skew angle on the live LDF of the simplified Henry's method (Huo *et al*., 2003; Huo and Zhang, 2008). In this study, a statistical analysis using a statistical computer program for the best fit based on the method of least squares (Dicleli and Erhan, 2009) was performed, to determine proper skew correction factor equations for the moment and shear (MCF and SCF, respectively) of MCB bridges.

11 Skew correction factor expression

The skew supports increase the value of the LDF of shear and reduce the maximum moment of bridges (Ebeido and Kennedy, 1996; Tobias *et al*., 2004; Bae and Oliva, 2012). Preliminary investigations indicated that the following parameters affect the skew correction factors of bridges: the ratio of L/d, the skew angle θ, and the web distances S. Therefore, using a statistical analysis, two established equations (Eqs. (4) and (5)) were used to modify the shear and moment distribution factor of the simplified Henry's method for skewed MCB bridges. These equations were in a similar form to the LRFD skew correction factor:

$$\mathrm{SCF}=1+\left(1.15+0.2\frac{L}{d}\right)\times 0.568(\tan\theta)^{0.27}S^{0.17}, \quad (4)$$

$$\mathrm{MCF}=1+\left(1.1+0.25\frac{L^2}{d^2}\right)(0.15-0.1\tan\theta)S^{0.15}. \quad (5)$$

A closer look revealed that the effect of the third term of the equations is insignificant (5% and 7.1%, respectively), so it can be underestimated.

Regression analysis was carried out to validate the proposed Eqs. (4) and (5). Figs. 8 and 9 show a

comparison between moment and shear obtained from a rigorous FEA and Henry's method with and without applying the proposed skew correction equations. The two proposed equations reduced the scattering of results as the coefficients of determinations R^2 of shear changed from 0.4856 to 0.7975, and from 0.6023 to 0.9260, respectively for the maximum bending moment, which indicates a slight deviation compared with rigorous analysis. The average values are equal to 1.068 and 1.110 for shear and moment, respectively, with corresponding standard deviations of 0.096% and 1.07%, which revealed the proposed equations do in fact determine acceptable results.

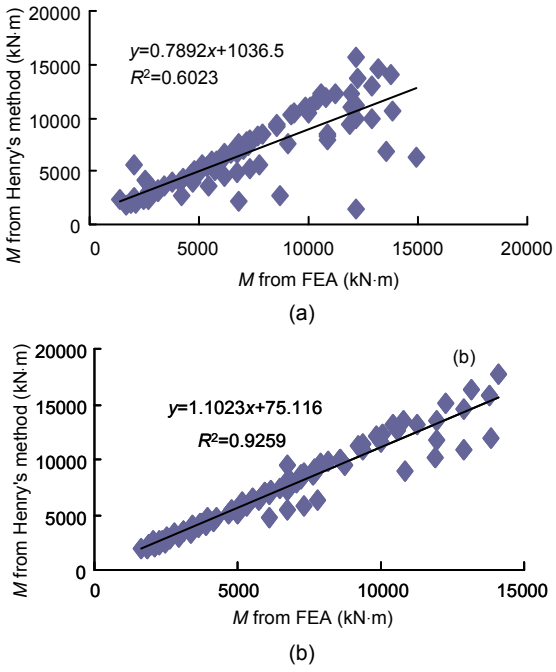

Fig. 9 Relationship between the bending moments determined by finite element analysis and by Henry's method, without (a) andwith (b) a skew correction factor

12 Secondary bending moment

Generally, the effect of torsional moment in the regions where the maximum bending moment is small can be underestimated. In skewed decks, torsion includes transverse and negative flexural bending that must be considered. Although the advanced finite element program is able to take these effects into consideration, they are often very time-consuming. Most specifications (e.g., LRFD and AASHTO specifications) and simplified methods (e.g., Henry's method) are unable to determine the secondary moments of bridges. Grillage analysis, which is a fast and reliable method, requires post-processing to determine the torsional moment of the superstructure that is partly confusing. To find a solution to this problem, the results of the FEA from a parametric study on prototype bridges (Table 1) were employed to obtain the ratio of the secondary moments (positive and negative torsions, negative moment) to the maximum bending moment obtained by the grillage analysis (Fig 10). Based on the upper bound envelopes of values, to keep a safe level due to the limited range of bridges, the following expressions were deduced.

Negative bending moment:

$$M^-=M^+(0.24\sin\theta+0.43),\quad 0°\le\theta\le30°, \tag{6}$$

$$M^-=M^+(1.775\sin\theta+0.34),\quad 30°\le\theta\le60°; \tag{7}$$

Positive torsional moment:

$$T^+=M^+(0.566\sin\theta+0.11),\quad 0°\le\theta\le60°; \tag{8}$$

Negative torsional moment:

$$T^-=M^+(0.127\sin\theta+0.12),\quad 0°\le\theta\le60°. \tag{9}$$

Fig. 10 shows that the magnitude of the secondary moment increases as the skew angle increases. The negative bending moments can be disregarded for skew angles of less than 30°. In cases with a high skew angle, due to the effects of torsion, the negative moment would be even more significant than the longitudinal bending moment. The proposed secondary moment (Eqs. (6) to (9)) gives the positive value that can be combined with the positive bending moment to obtain the most critical moment for bridge design of MCB bridges.

13 Conclusions

A sensitive study was performed on 90° skewed MCB bridges under traffic loading conditions. Based on the numerous data generated, the following conclusions can be made:

1. Torsional stiffness has a significant effect on

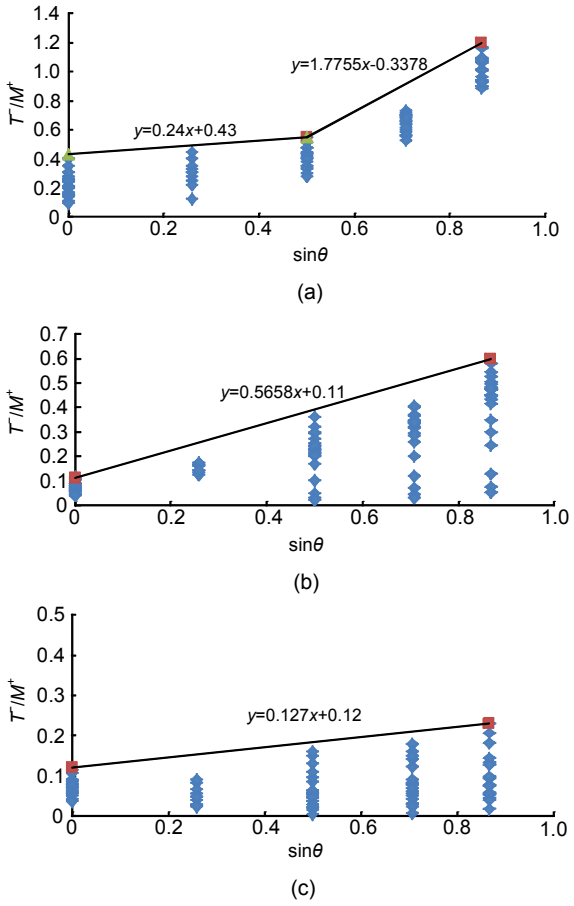

Fig. 10 Ratio of secondary moment to positive bending moment
(a) Negative bending moment; (b) Positive torsional; (c) Negative torsional moment

bridge actions. The effect of internal webs on torsional stiffness is negligible.

2. The twisting distribution at the obtuse corner is higher than that at the acute corner of skewed bridges and with an increasing skew angle, and the twisting moment at the girder increases significantly. However, in driving the live loads from one obtuse corner to another, the negative moment increases.

3. The proposed correction factors are able to predict the maximum LDFs of girders.

4. All of the secondary moments grow in magnitude with expanding skewness. The obtained equations for secondary moments are an excellent tool for bridge design procedure, especially at the initial level of design, in order to determine the appropriate reinforcement for the transverse direction of bridges.

References

AASHTO, 2002. Bridge Design Specifications. American Association of State Highway and Transportation Officials (14th Edition), Washington DC.

AASHTO, 2008. AASHTO LRFD Bridge Design Specifications: Customary US Units (5th Edition). American Association of State Highway and Transportation Officials, Washington DC.

Ashebo, D.B., Chan, T.H.T., Yu, L., 2007. Evaluation of dynamic loads on a skew box girder continuous bridge Part I: Field test and modal analysis. *Engineering Structures*, **29**(6):1052-1063. [doi:10.1016/j.engstruct.2006.07.014]

Bae, H.U., Oliva, M., 2012. Moment and shear load distribution factors for multigirder bridges subjected to overloads. *Journal of Bridge Engineering*, **17**(3):519-527. [doi:10.1061/(ASCE)BE.1943-5592.0000271]

Barker, R.M., Puckett, J.A., 1997. Design of Highway Bridges Based on AASHTO LRFD Bridge Design Specifications. John Wiley & Sons, New York, USA.

Begum, Z., 2010. Analysis and Behavior Investigations of Box Girder Bridges. MS Thesis, University of Maryland, USA.

CHBDC, 2000. Canadian Standards Association: Canadian Highway Bridge Design Code. CAN/CSA-S6-00, CSA International, Toronto, Ontario, Canada.

Chun, B.J., 2010. Skewed Bridge Behaviors: Experimental, Analytical, and Numerical Analysis. PhD Thesis, Wayne State University, USA.

Dicleli, M., Erhan, S., 2009. Live load distribution formulas for single-span prestressed concrete integral abutment bridge girders. *Journal of Bridge Engineering*, **14**(6):472-486. [doi:10.1061/(ASCE)BE.1943-5592.0000007]

Ebeido, T., Kennedy, J.B., 1996. Shear and reaction distributions in continuous skew composite bridges. *Journal of Bridge Engineering*, **1**(4):155-165. [doi:10.1061/(ASCE)1084-0702(1996)1:4(155)]

Euro-Code 2, 2005. European Standard: Design of Concrete Structures-Concrete Bridges: Design and Detailing Rules. London, UK.

Fan, Z., Helwig, T.A., 2002. Distortional loads and brace forces in steel box girders. *Journal of Structural Engineering*, **128**(6):710-718. [10.1061/(ASCE)0733-9445(2002)128:6(710)]

Foinquinos, R., Kuzmanovic, B., Vargas, L.M., 1997. Influence of Diaphragms on Live Load Distribution in Straight Multiple Steel Box Girder Bridges. Proceedings of 15th Structures Congress, ASCE, Portland. OR, USA, p.89-103.

Fu, C.C., Tang, Y., 2001. Torsional analysis for prestressed concrete multiple cell box. *Journal of Engineering Mechanics*, **127**(1):45-51. [doi:10.1061/(ASCE)0733-9399(2001)127:1(45)]

Hall, D., Grubb, M., Yoo, C., 1999. Improved Design Specifications for Horizontally Curved Steel Girder Highway

Bridges. National Cooperative Highway Research Program (NCHRP), Washington DC.

Hambly, E.C., 1991. Bridge Deck Behaviour (2nd Edition). Chapman & Hall, New York, NY.

Heins, C., 1978. Box girder bridge design state-of-the-art. *Engineering Journal of the American Institute of Steel Construction*, **15**(4):126-142.

Huo, X., Zhang, Q., 2008. Effect of skewness on the distribution of live load reaction at piers of skewed continuous bridges. *Journal of Bridge Engineering*, **13**(1):110-114. [doi:10.1061/(ASCE)1084-0702(2008)13:1(110)]

Huo, X., Conner, S., Iqbal, R., 2003. Re-Examination of the Simplified Method (Henry's Method) of Distribution Factors for Live Load Moment and Shear. Final Report, Tennessee DOT Project No. TNSPR-RES, 1218, USA.

Huo, X., Wasserman, E., Iqbal, R., 2005. Simplified method for calculating lateral distribution factors for live load shear. *Journal of Bridge Engineering*, **10**(5):544-554. [doi:10.1061/(ASCE)1084-0702(2005)10:5(544)]

Jaeger, L.G., Bakht, B., 1982. The grillage analogy in bridge analysis. *Canadian Journal of Civil Engineering*, **9**(2): 224-235. [doi:10.1139/l82-025]

Kolbrunner, C.F., Basler, K., 1969. Torsion in Structures: An Engineering Approach. Springer-Verlag, Berlin, p.1-21, 47-50.

Krätzig, W., 1993. Best transverse shearing and stretching shell theory for nonlinear finite element simulations. *Computer Methods in Applied Mechanics and Engineering*, **103**(1-2):135-160. [doi:10.1016/0045-7825(93)90043-W]

Park, N.H., Choi, S., Kang, Y.J., 2005. Exact distortional behavior and practical distortional analysis of multicell box girders using an expanded method. *Computers & Structures*, **83**(19-20):1607-1626. [doi:10.1016/j.compstruc.2005.01.003]

Razaqpur, A.G., Li, H., 1991. Thin-walled multicell box-girder finite element. *Journal of Structural Engineering*, **117**(10):2953-2971. [doi:10.1061/(ASCE)0733-9445(1991)117:10(2953)]

Sennah, K., Kennedy, J.B., 1999. Load distribution factors for composite multicell box girder bridges. *Journal of Bridge Engineering*, **4**(1):71-78. [doi:10.1061/(ASCE)1084-0702(1999)4:1(71)]

Song, S., Chai, Y., Hida, S., 2003. Live-load distribution factors for concrete box-girder bridges. *Journal of Bridge Engineering*, **8**(5):273-281. [doi:10.1061/(ASCE)1084-0702(2003)8:5(273)]

Théoret, P., Massicotte, B., Conciatori, D., 2012. Analysis and design of straight and skewed slab bridges. *Journal of Bridge Engineering*, **17**(2):289-301. [doi:10.1061/(ASCE)BE.1943-5592.0000249]

Tobias, D.H., Anderson, R.E., Khayyat, S.Y., Uzman, Z.B., Riechers, K.L., 2004. Simplified AASHTO load and resistance factor design girder live load distribution in Illinois. *Journal of Bridge Engineering*, **9**(6):606-613. [doi:10.1061/(ASCE)1084-0702(2004)9:6(606)]

Zhang, Q., 2008. Development of Skew Correction Factors for Live Load Shear and Reaction Distribution in Highway Bridge Design. PhD Thesis, Tennessee Technological University, Tennessee, USA.

Zokaie, T., Mish, K., Imbsen, R., 1993. Distribution of Wheel Loads on Highway Bridges, Phase III. NCHRP Final Report 12-26(2), Transportation Research Record, Washington DC.

Appendix A: Non-Orthogonal grillage method

The same procedure as recommended by Hambly (1991) was used to obtain the grillage layout and properties. The grid mesh is chosen with longitudinal members coincident with webs. Two nominal members are located along the edges of the cantilevers. The section is divided in such a way that each internal longitudinal member has half of the top and bottom slabs. The torsion constant and shear area in the longitudinal direction can be determined by the following equations, respectively:

$$c=\frac{2h^2d'd''}{(d'+d'')}\text{ per unit width,} \tag{A1}$$

$$A_s=W\cdot h, \tag{A2}$$

where h and W stand for depth and width of deck, and d' and d'' are the top and bottom thicknesses, respectively.

The transverse member represents the top and bottom slab and is perpendicular to the longitudinal members. The maximum spacing of transverse members is taken as one-quarter of the contra-flexure point's distance but the spacing is chosen to be shorter near the intermediate supports to give greater detail.

Hambly (1991) indicated that the moment of inertia (i_s) per unit width in the transverse direction is half of the torsional constant (c_s) and their equivalent shear area can be obtained by

$$a_s=\frac{d'+d''}{l^2}\left[\frac{d_w^3 l}{d_w^3+(d'^3+d''^3)h}\right]\frac{E}{G}\text{ per unit width,} \tag{A3}$$

where d_w, E and G are the thickness of web, the modulus of elasticity and shear modulus of bridge, respectively.

Appendix B: Simplified Henry's EDF method

Henry's EDF method requires only the roadway width (W_{roadway}), number of beams (N_{beam}) and an intensity factor (IF) based on a linear interpolation to determine the total number of traffic lanes considered as live load on the bridge. From the AASHTO Standard, the intensity factor of live load equals 100% for a two-lane bridge, 90% for a three-lane bridge, or 75% for a four-line or more lane bridge. Henry's EDF method for interior and exterior beams is as follows:

$$\mathrm{DF}=\frac{W_{\text{roadway}}}{10}\times \mathrm{IF}\times\left(\frac{2}{N_{\text{beam}}}\right).$$

The multicell box is considered as a group of equivalent I-beams based on the centre-to-centre distance between the webs. The number of equivalent I-beams is counted as the number of beams in the calculation.